Acquisition of kinematic and sEMG data from young and older adults using an upper limb exoskeleton*

Hellen Rivero-Pineda[1], Estefania Suarez-Perez[1], Manuela Gomez-Correa[2], Javier M. Antelis[3], Luis G. Hernández-Rojas[3], Mariana Ballesteros[2], David Cruz-Ortiz[1]

***Abstract*— This work describes the acquisition of kinematic and surface electromyography (sEMG) data from young and older adults during the execution of wrist movements using an upper limb rehabilitation robot (ULRR), along with a wristband equipped with inertial measurement units (IMUs) and sEMG sensors. These devices enable the observation of electrical muscle activation in the forearm during movement execution, providing valuable insights into the neuromuscular dynamics involved in motor control and movement mechanics. The description covers the robot configuration, sensor array, graphical user interfaces (GUIs) for visualizing robot data and biosignals, the experimental protocol, the database structure, and the signal processing and evaluation procedures. For the experimental protocol, 20 participants, 10 young and 10 older adults, were recruited. The test consisted of four basic wrist movements: radial deviation, ulnar deviation, flexion, and extension, which were performed in random order under the guidance of the ULRR GUI. The sEMG analysis indicated that older adults tend to overuse specific muscles and exhibit a higher percentage of compensatory movements (38.5%) than younger participants (24.25%). The study's findings enable the identification of age-related differences in muscle activation and compensation, aiding the design of personalized rehabilitation programs and improved devices to enhance motor function in older adults.**

***Index Terms*— sEGM system, Robotic rehabilitation, Motor disability, Older adults**

I. INTRODUCTION

Motor skills are defined as the ability to perform coordinated and precise bodily movements, allowing actions to be carried out smoothly and synchronously. Motor abilities depend on factors such as practice conditions, task-specific demands, and individual characteristics of the performer. It is generally considered an innate trait, relatively stable and enduring over time, providing the foundation necessary for the development and execution of a wide range of motor and cognitive skills [1]. However, with aging, there is a progressive deterioration of these skills and motor control, which can significantly compromise functionality and autonomy [2]. Several factors influencing motor performance are related to bodily changes occurring during aging, such as muscle strength loss, reduced joint flexibility, and sensory acuity deterioration [3]. While various neuromuscular physiological factors determine motor performance, neuroimaging studies have revealed that cognitive and motor functions are closely interconnected, sharing standard neural mechanisms and resources [4]. This relationship is evident in older adults through slower movement initiation, especially in the dominant hand, which is linked to increased theta wave activity and reduced functional connectivity in the sensorimotor cortex. These changes suggest a shared neural mechanism contributing to muscle deterioration (sarcopenia) and cognitive decline, highlighting the connection between physical health and brain function in aging [5].

Although various factors affecting motor performance have been identified, the variability in the execution of motor responses in older adults remains not fully understood. Therefore, it is crucial to have metrics that allow for an objective assessment of motor performance and functioning in this population. The evaluation of upper limb motricity has been established as a quantitative test that analyzes both active and passive movements and the sensory ability to perform goal-directed movements. Key evaluation criteria include range of motion, muscle strength, coordination, motor control, and functional dexterity [6]. These assessments have been enriched by advanced technologies such as inertial measurement units (IMUs), computer vision-based motion analysis systems, and surface electromyography (sEMG) sensors. The latter allows the recording of electrical activity resulting from the summation of action potentials from active motor units [7]. However, to achieve a more detailed assessment of movement kinematics, it is essential to integrate complementary technologies that work simultaneously, enabling a deeper analysis of motor control mechanisms.

In this context, robotic devices have emerged as key tools, as they not only facilitate precise and quantitative measurements of motor performance during task execution but also enable objective evaluations within rehabilitation processes. The data obtained from robots are valuable for both therapeutic strategy design and research on neuroplasticity [8]. Furthermore, robot-assisted rehabilitation plays a crucial role in motor function recovery, helping to prevent deterioration, improve strength, restore lost functions, and maintain functional autonomy [9]. To promote independent living in older adults, robotic systems in both clinical and

*This work was partly supported by the Instituto Politécnico Nacional under Grants: SIP-20250223 and SIP-20250253. The authors thank the support provided by Secretaría de Educación, Ciencia, Tecnología e Innovación de la Ciudad de México (SECTEI) under the grant SECTEI/081/2024.

[1]Medical Robotics and Biosignals Lab, UPIBI, Instituto Politécnico Nacional, Av. Acueducto, La Laguna Ticoman, Gustavo A. Madero, 07340, Mexico City, Mexico. email: hriverop1700@alumno.ipn.mx, esuarezp1900@alumno.ipn.mx and dcruzo@ipn.mx.

[2]Medical Robotics and Biosignals Lab, CIDETEC, Instituto Politécnico Nacional, Gustavo A. Madero, Mexico City. email: mgomezc2103@alumno.ipn.mx and mballesterose@ipn.mx.

[3]Tecnologico de Monterrey, Av. Gral Ramón Corona No 2514, Colonia Nuevo México, 45201, Zapopan, México. email: mauricio.antelis@tec.mx and luisg.hernandez@tec.mx.

home settings have increased [10]. However, there remains a gap in research focused on the specific evaluation of older adults using these technologies. Therefore, it is essential to analyze the metrics derived from robotic devices to fully understand their long-term benefits and potential limitations, advancing toward developing personalized and effective therapeutic protocols [11].

Based on the above, the present study aims to collect kinematic data and sEMG signals from a group of young and older adults during the execution of basic hand movements, such as flexion, extension, and ulnar and radial deviation, using a robotic upper limb rehabilitation device, IMUs, and sEMG. The goal is to perform a quantitative and comparative analysis of different kinematic and sEMG parameters to identify differences between the two age groups when using rehabilitation technologies, considering the mobility loss associated with aging. This research represents the first phase of a broader project developing personalized rehabilitation systems tailored to each patient's needs.

II. System Description

The system integrates two subsystems and two software components to acquire and process biosignals and kinematic data through an upper limb rehabilitation robot (ULRR). This combination enables the assessment of the forearm muscle's dynamics and electrical activity during wrist flexion-extension (WFE) and wrist radial-ulnar deviation (WRU) movements performed using the ULRR.

The first subsystem connects the ULRR to a graphical user interface (GUI), randomly displaying specific markers, allowing the user to guide their wrist movements toward the presented target. Meanwhile, the second subsystem links another GUI to a wristband equipped with four sEMG sensors, which capture the electrical signals of the targeted muscles, and two inertial measurement units (IMUs), which record the trial's kinematic data via a WiFi connection.

A. Robot configuration

The proposed ULRR was based on four anthropometric measurements of the upper limbs from the adult Mexican population: arm length, forearm length, hand length, and hand width. Additionally, four degrees of freedom (DoF) were incorporated, as the focus was on four joints of the upper limb: elbow flexion/extension (EFE), WRU, WFE, and wrist pronation/supination (WPS). Please refer to the work in [12] for further details. Notice that for this work we only considered WRU and WFE movements.

1) Structural design: Figure 1 shows the standard configuration of the robot, which consists of five main segments. The first one is a metallic base made from aluminum profiles that support the weight of the ULRR and the user's upper limb. The other four segments are the components that comprise each DoF in the ULRR. In this representation, the WRU joint is shown in purple (see Figure 1.i), the EFE in yellow (see Figure 1.ii), the WFE in orange (see Figure 1.iii), and the WPS in blue (see Figure 1.iv). These pieces were fabricated using three-dimensional (3D) printing techniques with polylactic acid (PLA) filament.

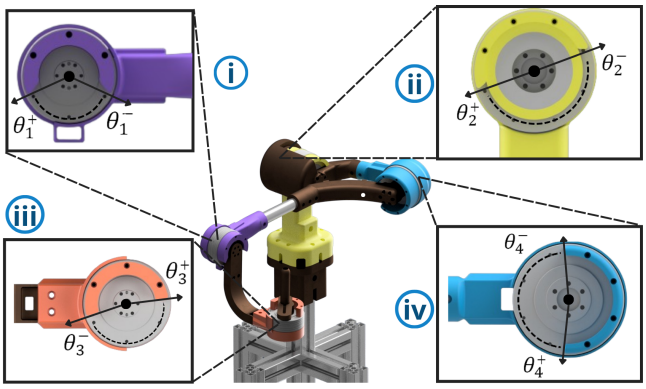

Fig. 1. ULRR Structural design.

2) Electronic instrumentation: The electronic design of the ULRR includes four 24 V CubeMars® brushless motors, with a control board that incorporates a 14-bit absolute encoder, providing an angular resolution of 0.1 deg. The microcontroller used was a Texas Instruments TM Launchpad F28379xD, as it features a dual-core design that provides 32-bit processing capabilities. It includes a controller area network (CAN) module, a serial communication protocol for control applications, and supports bit rates of up to 1 Mbit/s. This microcontroller collects each joint's position and velocity data and sends it to the data store in the MATLAB® environment.

B. Biosignals modules

The biosignal acquisition system comprises two modules with two sEMG sensors, an IMU and a microcontroller, as shown in Figure 2. Each module has two Gravity Analog sEMG sensors (see Figure 2.i), which amplify minimal sEMG within 1.5 mV 1000 times, with an analog output signal and takes 1.5 V as a reference with an output voltage range extends from 0 to 3.3 V (see Figure 2.ii). The IMU is composed of a board that contains an LSM6DSOX + LIS3MDL sensors (see Figure 2.iii), which includes nine DoF: three degrees for the accelerometer, three for the gyroscope, and the last three for the magnetometer.

The accelerometer uses a range of ± 16 g (± 156.96 m/s^2), and the gyroscope is operating with ± 2000 deg/s (± 34.9066 rad/s). The LIS3MDL magnetometer sensor provides data regarding the direction of the strongest magnetic force and was configured with a range of ± 12 G (± 0.0012 T).

To acquire the signals, a FireBeetle ESP-32 microcontroller (see Figure 2.iv) was used, which connects to a WiFi network and communicates through user datagram protocol (UDP). The microcontroller sends the acquired values from the sensors to the interface that displays the sEMG signals when it receives a UDP packet. Also, the module is powered by a 3.7 V, 400 mAh Li-Po battery (see Figure 2.v). To facilitate the placement of the sensors, a velcro bracelet was used (see Figure 2.vi), where the two microcontrollers with their respective sensors were placed.

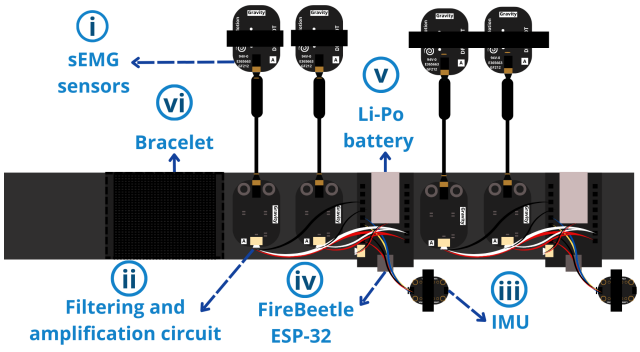

Fig. 2. Acquisition armband and its components.

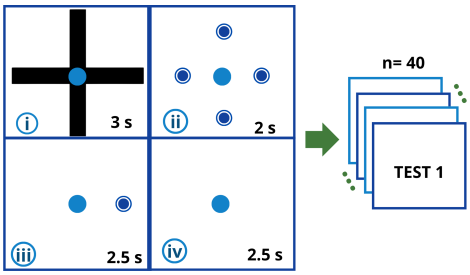

Fig. 3. Parameters evaluated in the test.

III. Software Description

The software comprises two GUIs, one for the robot and one for the biosignals acquisition.

A. Robot interface

The software that enables the connection between the ULRR and the user is based on a GUI developed using MATLAB's App Designer tool. This interface displays visual stimuli through markers specifying the direction in which the WRU and WFE movements should be performed. Additionally, it facilitates the acquisition, monitoring, and storage of position and velocity data from the WFE and WRU motors during the user's movements.

The interface development consists of three main stages: 1) configuration and acquisition, 2) marker visualization, and 3) storage. The subsections of the GUI are described as follows:

1) Configuration and acquisition: Before using the device, the motor positions are calibrated to zero to obtain measurements from a reference. The data is sent to the microcontroller through a communication port, and a response of a specific length is expected. Once received, the data is verified, decoded, and processed to extract position and velocity to control and monitor the device.

2) Marker visualization: An algorithm was developed to present the stimuli for a predetermined duration. Figure 3 shows the four phases of each trial period: i) Rest, ii) Visual Stimulus, iii) Target Marker, and iv) Centering. A black cross and the central marker are displayed during phase (i) for 3 seconds (see Figure 3.i). In stage (ii), the visual stimulus is presented with markers in the four possible directions (up, down, left, and right), along with the central marker, for 2 seconds (see Figure 3.ii). In (iii), three of the markers disappear, and only the marker indicating the direction of the movement to be performed is displayed randomly for 2.5 seconds (see Figure 3.iii). Finally, the central marker is shown in stage (iv), signaling the movement towards the central position for 2.5 seconds (see Figure 3.iv).

3) Storage: The data is stored by obtaining the position vectors, speed, time, and position of the randomly displayed marker during each repetition. These data are saved in .mat files, segmented and labeled into separate columns for each repetition, resulting in 40 columns containing a specific number of data points.

B. Biosignals interface

The data acquisition, visualization, and storage software was developed through an interface in Node-RED, a flow-based programming tool based on JavaScript. The interface has three sections necessary to obtain the information: 1) configuration, 2) modules connection, and 3) acquisition. Each of these is described below.

1) Configuration: In this network configuration section, the user has to enter the WiFi network to which the computer is connected in the service set identifier (SSID) text box. The network password is entered in the password text box, and then the user proceeds to save the information, which opens the next section for the user.

2) Modules connection: In this stage, the modules are connected through serial communication, selecting the port to which the microcontroller is connected. The above sends the network information and the UDP port of the module to the microcontroller. Once the connection has been established, a red LED changes to green, indicating the connection succeeded. When the two modules have been connected, the user selects the save button to open the last section.

3) Acquisition: Finally, at this point, the system works with the UDP protocol, and the user can use the bracelet. In this section, the file's name and the folder address where the data will be stored can be specified; the software generates a CSV file with the sensors' information at the end of the test. Also, the GUI displays the four graphs corresponding to the sEMG sensors online.

IV. System Synchronization

Both data acquisition systems must be connected to the same WiFi network before and during program execution. Synchronization of the systems is performed using a network communication protocol based on an internet protocol (IP) address. In the ULRR system software, the computer's IP address where the biosignal interface is located must be entered. Once the IP address is set and the robot interface program is executed, the synchronization is established, which works through interruptions or digital flags, when the first program (robot GUI) sends a "0" to the second program (biosignal GUI) both start the acquisition of information and its storage. Then, when the first program finishes its acquisition it sends a "1" to the second program indicating the end of the data storage, saving each program in its respective computer the information obtained.

V. Experimental protocol

A. Participants

The participants' selection excluded those with self-reported mobility-restricting pathologies in the wrist, arm, or hand and those with musculoskeletal diseases. A total of 20 subjects (10 young adults and 10 older adults) signed informed consent and participated in the study. Also, half of the participants are women, and half are men. The young adults' ages range between 20 and 34 years, and the older adults are between 60 and 78 years old. The protocol study was approved by the research ethics committee of Instituto Tecnológico y de Estudios Superiores de Monterrey (No. 20250223). The tests were conducted at the Medical Robotics and Biosignals Laboratory, Instituto Politécnico Nacional.

B. System setup

General information is gathered, such as age, gender, and demographic details, including occupation and lifestyle factors such as physical activity frequency. Then, the anatomical measurements of both arms were measured, such as arm length, forearm length, maximum arm circumference, mid-arm circumference, minimum arm circumference, maximum forearm circumference, mid-forearm circumference, minimum forearm circumference, palm length, and palm width.

Once the general information has been recorded, the participants have five minutes to familiarize themselves with the robot and the interface. Subsequently, all the elements contemplated in the acquisition protocol are placed and activated, as shown in Figure 4.

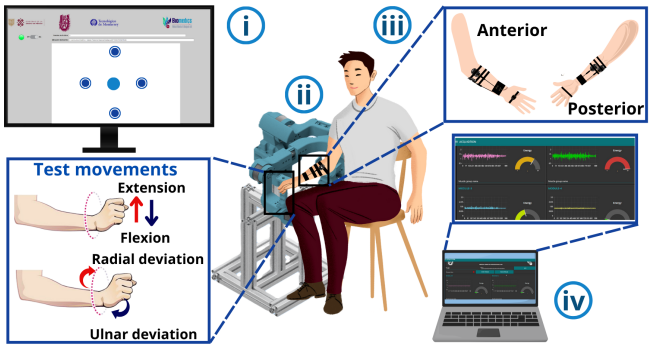

Fig. 4. Integrating subsystems.

For user preparation, the right arm is cleaned with alcohol to remove substances that may interfere with the signal acquisition, and the operation of the sensors is verified in the sEMG GUI (see Figure 4.iii and Figure 4.iv). Furthermore, the Gravity sEMG sensors are attached to the participant's right hand, regardless of laterality, and placed on the muscles: extensor carpi radialis (see Figure 5.i), extensor carpi ulnaris and extensor digitorum (see Figure 5.ii), extensor carpi radialis longus (see Figure 5.iii) and palmaris longus (see Figure 5.iv). The sensors were attached using straps to ensure correct surface contact with the skin. Also, the sample rate established for the sEMG sensors was 850 Hz and 85 Hz for the IMU's variables [13].

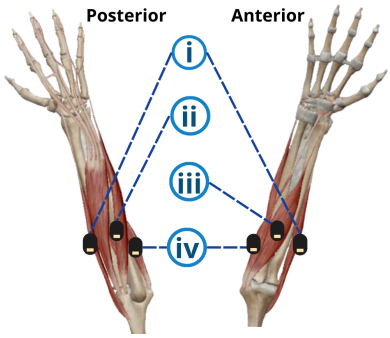

Fig. 5. Gravity sEMG sensors placement on right arm.

Then, each participant is seated half a meter away from the screen, where the interface is visible, and their arm is attached to a four DoF robotic device, as shown in Figure 4.ii. When the system's operation is verified, the test starts by activating the interface shown in Figure 4.i, which also synchronizes the systems and stores the information of interest. This process is repeated with the two experiments mentioned in Section V-C.

C. Experiment design

The experimental design consists of two stages. The first stage encompasses a generalized range of motion, defined as a displacement of ± 52.5 degrees for WFE and 30 degrees for WRU. The second stage adapts the individual subject's maximum and minimum ranges of motion. For this, the user is asked to perform three effortless repetitions of the four basic movements, and the highest value ranges are saved to adjust the robot GUI to the user's custom values.

In each of the stages, the phases shown in Figure 3 were repeated until each target marker was displayed 10 times in random order, which means that at the end of each test, the participants executed 10 wrist flexions, 10 extensions, 10 ulnar deviations, and 10 radial deviations, resulting in 40 repetitions of the test.

VI. Signals evaluation

A. Database configuration

Once the data had been recorded using the protocol described in the previous section, the database structure was selected. Figure 6 illustrates the database's conformation.

The database consists of folders where the signals are stored for each subject. Subsequently, each folder contains two main subsections: segmented and raw data. In addition, a metadata file was appended in which participant information such as age, generation, and physical activity was included.

The raw data folder contains 27 files, each containing information for one run, 40 consecutive trials. These files correspond to the four sEMG signals, the nine variables of each IMU (18 in total, considering that the system has two IMUs), the position and speed of each motor (four in total, considering that the robot use two motors), and finally, a

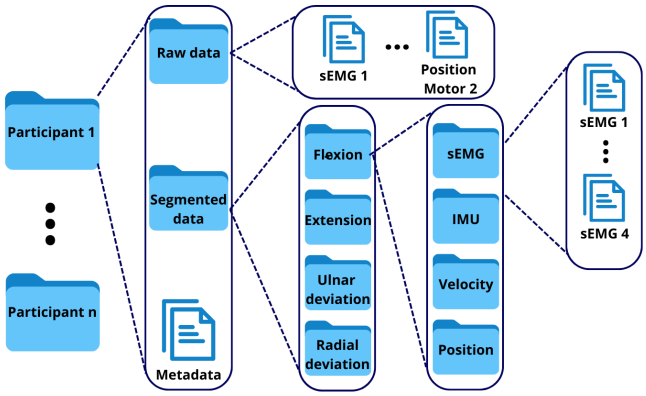

Fig. 6. Database structure.

vector indicating the random order of the movements for the test.

On the other hand, the segmented data contains four folders, in which the signals were divided according to the movement performed in each trial. Then, inside each movement folder, four folders were added according to the type of information recorded, thus obtaining a folder for sEMG signals, one for IMU signals, one for angular position, and finally, one for angular velocity. In these folders are 26 files (4 sEMG, 18 IMU variables, and four motor variables), and each file contains the time vector (ranging from 0 to 10 s) and the corresponding signal.

B. Data analysis

After collecting and segmenting the data for each participant in our database, an analysis was conducted to interpret their performance. For sEMG signals, an analysis to describe their characteristics in the time domain was computed. The following parameters were used: power (P), which provides information about muscle activation; root mean square (RMS), which indicates constant force and non-fatiguing contraction; waveform length (WL); and slope sign change (SSC), which represents the number of times the slope of the EMG signal changes sign. For more details on the equations used, see the following papers [14]-[15].

On the other hand, the percentage of movements where the participants present compensating movements (for example, when, for the execution of WRU, the users generate a movement of WFE to reach the target) was estimated. The compensating movements were defined where the magnitude of the signal of the opposite axis presents a range out of ± 3 deg. The positions used correspond to the data recorded directly by the ULRR without applying any prior processing. For graphical representation, angular displacement was plotted using the x-axis, corresponding to WFE movements, and the y-axis, associated with WRU. As a result, a cross-shaped graph was obtained, reflecting the movements performed during the test and allowing visualization of the recorded trajectories for both study groups (young adults and older adults).

VII. Results and Discussion

Table I shows that for the first sEMG sensor (E1: extensor carpi ulnaris and extensor digitorum), the major part of the results obtained for the parameters (P, RMS, WL and SSC) evaluated in each movement (R: radial deviation, U: ulnar deviation, E: extension and F: flexion) the value corresponding to the older adults is higher than that of the young adults. The second sEMG sensor (E2: palmaris longus) shows a similar behavior concerning all the parameters and movements for older adults and young adults, with a minor difference between the values, except for the P in R and F movements, where the value for young adults is higher. In the third EMG sensor (E3: flexor carpi ulnaris) we observed that for the movements R, U, E, and F in the parameters P, RMS, WL, and SSC, the values of young adults are higher than those of older adults, except in F for WL and SSC which occur the other way around. Finally, it was observed that in the fourth sensor (E4: extensor carpi radialis longus) for the movements R, U, and E in the parameters P, RMS, and WL, the values of the young adults are greater than those of the older adults. In the parameter SSC, this is the other way around in these movements, and in F for the four parameters, the values of the older adults are greater than those of the young adults. The above means that young adults activated different muscles groups depending on the movements but in older adults the E1 is crucial for the execution of all the different movements.

TABLE I
Surface EMG parameters

		P		RMS		WL		SSC	
		Y	O	Y	O	Y	O	Y	O
R	E1	0.0018	0.0036	0.0370	0.0524	149.43	235.69	434.64	802.30
	E2	0.0011	0.0008	0.0253	0.0256	104.35	117.46	236.90	399.76
	E3	0.0005	0.0002	0.0184	0.0137	67.12	56.15	81.92	43.51
	E4	0.0006	0.0003	0.0202	0.0166	72.27	67.04	83.43	104.11
U	E1	0.0009	0.0010	0.0271	0.0281	111.65	134.21	264.93	440.78
	E2	0.0012	0.0012	0.0277	0.0307	114.17	139.21	283.73	550.91
	E3	0.0007	0.0002	0.0191	0.0139	64.24	55.51	46.01	38.71
	E4	0.0014	0.0004	0.0300	0.0181	99.73	74.23	133.48	143.68
E	E1	0.0019	0.0058	0.0404	0.0694	161.27	287.46	522.91	930.65
	E2	0.0015	0.0017	0.0312	0.0380	131.19	169.37	394.56	676.67
	E3	0.0005	0.0002	0.0183	0.0144	66.89	60.82	78.93	51.03
	E4	0.0006	0.0004	0.0210	0.0175	75.58	72.17	71.30	123.61
F	E1	0.0008	0.0012	0.0244	0.0309	101.38	148.01	196.83	489.26
	E2	0.0009	0.0008	0.0236	0.0246	96.97	113.63	184.70	371.48
	E3	0.0005	0.0004	0.0183	0.0176	68.15	72.08	79.84	140.99
	E4	0.0007	0.0008	0.0223	0.0253	81.66	101.49	106.57	306.16

Based on the segmentation obtained from the database, a comparison was conducted between young adults and older adults through a graphical analysis of the angular ranges achieved during WFE and WRU movements. Figure 7 presents the movement trajectories obtained for both populations. Older adults were observed to execute movement sequences with less precision than young adults and exhibited more restricted and variable angular ranges. Also, older adults present compensating movements in 38.5% of the test, whereas young adults present compensating movements in 24.25% of the total tests. The limited ability to perform and/or learn the motor sequences assessed in the test may have been influenced by various factors, such as movement duration, DoF, cognitive feedback conditions derived from

the interaction between visual stimuli and movement execution, as well as the cognitive-motor control processes required for a more precise execution.

This performance may be affected by various aging-related conditions, including reduced muscle strength and diminished sensory activity in vision and tactile perception. At the neuromuscular level, alterations such as sarcopenia and morphological changes in the motor unit and its neural inputs result in slower and more variable contractile velocity, fatigue increased, and reduced stability of synaptic inputs, all of which contribute to the decline in motor performance among older adults [16].

Another variable influencing performance is related to differences in central information processing between older and younger adults. This performance is closely linked to a lower perception observed in the older population. To mitigate the impact of this natural aging phenomenon on the test, participants were allowed to familiarize themselves in advance with the interface and the use of the ULRR. Since learning and executing these motor sequences require the perception of spatial positions of the targets before and during the test, this familiarization facilitated the selection and execution of responses within a limited time window. However, the results obtained show variations between the analyzed groups. In future work, additional assessments and metrics will be conducted based on the data collected to further analyze the findings.

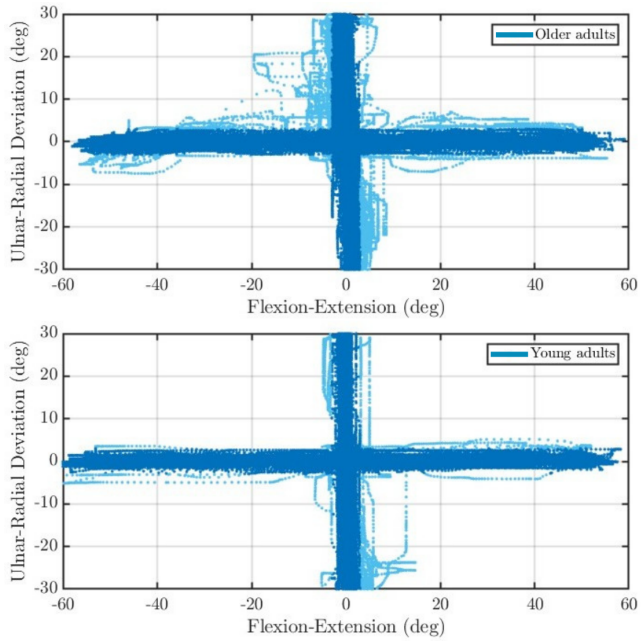

Fig. 7. Position trajectories during hand movement.

VIII. Conclusion

In the present work, sEMG signals and kinetic data were acquired from older and young adults using an ULRR to execute basic hand movements. From the information collected, older adults presented compensating movements in 38.5% of the trajectories obtained in average compared with a 24.25% from young adults. In addition the sEMG data analysis suggested that the movement performed by older adults directly depends on the activation of extensor carpi ulnaris and extensor digitorum while young adults activate different muscles depending on the executed movement.This study was conducted as the first step in analyzing this type of rehabilitation system in different populations to identify the requirements or needs of different groups of patients and generate user-based therapies.

References

[1] H. Sveistrup, P. A. Burtner, and M. H. Woollacott, "Two motor control approaches that may help to identify and teach children with motor impairments," *Pediatric Exercise Science*, vol. 4, no. 3, pp. 249–269, 1992.

[2] M. E. Perry, C. R. McDonald, D. J. Hagler, L. Gharapetian, J. M. Kuperman, A. K. Koyama, A. M. Dale, and L. K. McEvoy, "White matter tracts associated with set-shifting in healthy aging," *Neuropsychologia*, vol. 47, no. 13, pp. 2835–2842, 2009.

[3] M. Gallou-Guyot, S. Mandigout, L. Combourieu-Donnezan, L. Bherer, and A. Perrochon, "Cognitive and physical impact of cognitive-motor dual-task training in cognitively impaired older adults: An overview," *Neurophysiologie Clinique*, vol. 50, no. 6, pp. 441–453, 2020.

[4] T. Ogawa, H. Shimobayashi, J.-I. Hirayama, and M. Kawanabe, "Asymmetric directed functional connectivity within the frontoparietal motor network during motor imagery and execution," *Neuroimage*, vol. 247, p. 118794, 2022.

[5] N. S. Frolov, E. N. Pitsik, V. A. Maksimenko, V. V. Grubov, A. R. Kiselev, Z. Wang, and A. E. Hramov, "Age-related slowing down in the motor initiation in elderly adults," *Plos one*, vol. 15, no. 9, p. e0233942, 2020.

[6] Y. Ueyama, T. Takebayashi, K. Takeuchi, M. Yamazaki, K. Hanada, Y. Okita, and S. Shimada, "Attempt to make the upper-limb item of objective fugl–meyer assessment using 9-axis motion sensors," *Sensors*, vol. 23, no. 11, p. 5213, 2023.

[7] J. V. Basmajian, "Muscles alive," *Their functions revealed by electromyography*, 1985.

[8] L. Zollo, L. Rossini, M. Bravi, G. Magrone, S. Sterzi, and E. Guglielmelli, "Quantitative evaluation of upper-limb motor control in robot-aided rehabilitation," *Medical & biological engineering & computing*, vol. 49, pp. 1131–1144, 2011.

[9] D. J. Stott and T. J. Quinn, "Principles of rehabilitation of older people," *Medicine*, vol. 45, no. 1, pp. 1–5, 2017.

[10] H. Melkas, L. Hennala, S. Pekkarinen, and V. Kyrki, "Impacts of robot implementation on care personnel and clients in elderly-care institutions," *International Journal of Medical Informatics*, vol. 134, p. 104041, 2020.

[11] S. Hussain, P. K. Jamwal, P. Van Vliet, and M. H. Ghayesh, "State-of-the-art robotic devices for wrist rehabilitation: Design and control aspects," *IEEE Transactions on human-machine systems*, vol. 50, no. 5, pp. 361–372, 2020.

[12] L. Leduc, M. Gomez-Correa, M. Ballesteros, and D. Cruz-Ortiz, "Robust control of a four dof rehabilitation robot for upper limb: A digital shadow approach," in *2024 12th International Conference on Control, Mechatronics and Automation (ICCMA)*, pp. 119–124, IEEE, 2024.

[13] M. Al-Ayyad, H. A. Owida, R. De Fazio, B. Al-Naami, and P. Visconti, "Electromyography monitoring systems in rehabilitation: A review of clinical applications, wearable devices and signal acquisition methodologies," *Electronics*, vol. 12, no. 7, p. 1520, 2023.

[14] A. Phinyomark, P. Phukpattaranont, and C. Limsakul, "Feature reduction and selection for emg signal classification," *Expert Systems with Applications*, vol. 39, no. 8, pp. 7420–7431, 2012.

[15] A. Sultana, F. Ahmed, and M. S. Alam, "A systematic review on surface electromyography-based classification system for identifying hand and finger movements," *Healthcare Analytics*, vol. 3, p. 100126, 2023.

[16] J. Vieweg, S. Panzer, and S. Schaefer, "Effects of age simulation and age on motor sequence learning: Interaction of age-related cognitive and motor decline," *Human Movement Science*, vol. 87, p. 103025, 2023.